Channel Estimation for Frequency-Domain Equalization of Single Carrier Broadband Wireless Communications

Y. Rosa Zheng
Missouri University of Science and Technology, zhengyr@mst.edu

Chengshan Xiao
Missouri University of Science and Technology, xiaoc@mst.edu

Channel Estimation for Frequency-Domain Equalization of Single Carrier Broadband Wireless Communications

Yahong Rosa Zheng, *Member, IEEE,* and Chengshan Xiao, *Senior Member, IEEE,*

***Abstract*— Frequency-domain equalization (FDE) is an effective technique for high data rate wireless communication systems suffering from very long intersymbol interference. Most of existing FDE algorithms are limited to slow time-varying fading channels due to lack of accurate channel estimator. In this paper, we employ interpolation method to propose new algorithms for frequency-domain channel estimation for both slow and fast time-varying fading. We show that least squares-based channel estimation and minimum mean square error-based channel estimation with interpolations are equivalent under certain conditions. Noise variance estimation and channel equalization in the frequency domain are also discussed with fine-tuned formulas. Numerical examples indicate that the new algorithms perform very well for severe fading channels with long delay spread and high Doppler spread. It is also shown that our new algorithms outperform recently developed frequency-domain least mean squares (LMS) and recursive least squares (RLS) algorithms which are capable of dealing with moderate fading channels.**

I. Introduction

Single carrier frequency-domain equalization (SC-FDE) has been shown to be an attractive equalization scheme for broadband wireless channels which has very long impulse response memory. Compared to orthogonal frequency division multiplex (OFDM), a single carrier system with FDE has similar performance and signal processing complexity but lower peak-to-average power ratio and less sensitivity to carrier frequency errors [4], and this arises from the use of single carrier modulation [5], [7]. Moreover, compared to time-domain equalization, SC-FDE has less computational complexity and better convergence properties [1] to achieve the same or better performance in severe frequency-selective fading channels.

Recent years, SC-FDE has received increasing attention in the literature [2]-[19]. Among the existing techniques, SC-FDE is often designed according to one of the following four channel assumptions: 1) the fading channel coefficients are assumed to be perfectly known at the receiver [6], [8], [10], [12], [15], [17], [18], then frequency-domain linear equalizers or decision feedback equalizers are analyzed and/or designed accordingly; 2) the fading channel are assumed to be constant for a frame consisting of one training block and many data blocks, the fading channel is estimated via the training block and utilized for equalization for the entire frame [2], [3], [4], without adaptive receiver processing; 3) the fading channel is assumed to be static for at least one block but varying within a frame, which consists a few training blocks (at the beginning of the frame) and many data blocks, then adaptive FDE is developed by employing least mean squares (LMS) or recursive least squares (RLS) adaptive processing in the frequency domain [5], [16], [19]; 4) the fading channel is assumed to be static for one block but varying from one block to another, then decision directed technique is utilized for channel estimation and equalization for DS-CDMA systems [14]. The equalizers developed based on the first two assumptions have demonstrated significant performance gain of frequency-domain equalization over time-domain equalization, however, they may not be applicable to practical systems over time-varying channels with satisfactory performance. The adaptive equalizers derived from the last two assumptions have achieved substantial advancement in dealing with slow time-varying frequency-selective channels compared with these non-adaptive SC-FDEs. However, as indicated in the examples of [5], [16], [19], the adaptive SC-FDEs employing LMS or RLS algorithms can degrade significantly for fast moving mobiles, which cause large Doppler spread leading to fast time-varying fading.

In this paper, we employ interpolation method to propose a new algorithm for frequency-domain channel estimation for severe time-varying and frequency-selective fading channels. Our new algorithms are developed by employing a frame structure which consists of one training block and many data blocks. The training block is utilized to estimate fading channel transfer function of the block. The fading channel transfer functions of the data blocks are estimated by interpolating the channel transfer functions of the training blocks at the current frame and the next frame. Noise variance is also estimated at the training blocks. Channel equalization is performed in the frequency domain by employing the estimated channel transfer functions and noise variance. This channel estimation method is similar to the time-domain interpolation method in [26], [27], but differs in that it is performed in frequency domain and can deal with both fast time-varying fading and severe intersymbol interference. Compared with the existing FD LMS and RLS algorithms, the proposed new method can deal with much larger Doppler spread fading with the same bit error rate and data efficiency.

The rest of the paper is organized as follows. Section II describes the system models and preliminaries. Section III presents the frequency-domain channel estimation and noise variance estimation. Section IV details the frequency-domain channel equalization. Section V illustrates numerical examples and Section VI draws the conclusion.

Manuscript received March 6, 2007; revised October 22, 2007 and December 31, 2007; accepted March 4, 2008. The editor coordinating the review of this paper and approving it for publication is A. Ghrayeb. This work was supported in part by the National Science Foundation under Grant CCF-0514770 and the Office of Naval Research under Grant N00014-07-1-0219.

The authors are is with the Department of Electrical and Computer Engineering, Missouri University of Science and Technology, Rolla, MO 65409 USA (e-mail: {zhengyr,xiaoc}@mst.edu).

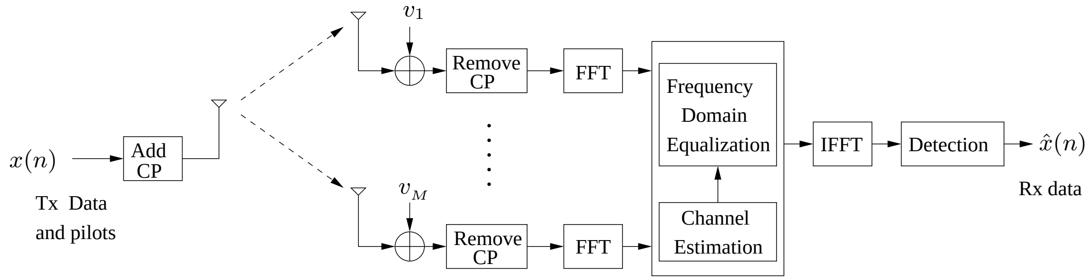

Fig. 1. The simplified block diagram of a single carrier SIMO wireless system with frequency-domain channel estimation and equalization.

II. System Model and Preliminaries

Consider a SIMO system with one transmit antenna and M receive antennas whose baseband equivalent model is shown in Fig. 1. At the transmitter, cyclic prefix (CP) is periodically added to the baseband data sequence $\{x(n)\}$ and modulated onto a single carrier frequency for transmission across the time-varying and frequency-selective fading channel. At the receiver, the CP is removed at each branch. The fast Fourier transform (FFT) is utilized to convert the time-domain data signal to the frequency-domain signal. Then frequency-domain channel estimation, equalization, and diversity combining are employed to mitigate inter-symbol interference. Finally an inverse FFT (IFFT) is equipped to convert the frequency-domain signal to time-domain signal for detection and estimation. The output is the estimated data sequence $\{\hat{x}(n)\}$.

To facilitate frequency-domain channel estimation and channel equalization for broadband wireless systems over time-varying and frequency-selective fading channels, we employ a data structure as shown in Fig. 2. The baseband signal sequence is partitioned into frames with each frame containing N_b signal blocks. The first block is a training block designed for channel estimation and noise variance estimation and the other (N_b-1) blocks are data blocks. Each block contains N_c symbols of CP and N symbols of data (or training) sequence. The block time duration is $T_b = (N_c + N)T_s$, and frame duration is $T_f = N_b(N_c + N)T_s$, where T_s is the symbol period.

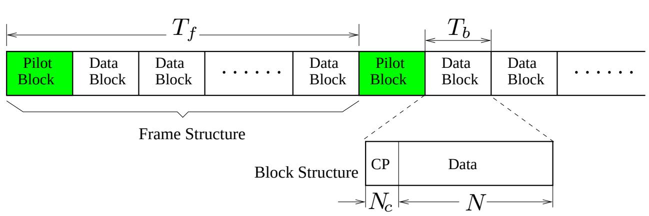

Fig. 2. The frame structure.

A. Time-Domain System Model

Let $x_p(n)$ be the n-th transmitted symbol at the p-th block of the current frame, $y_{p,m}(n)$ be the n-th received baseband signal in the p-th block of the current frame at the m-th receive branch. Then the received baseband signal is given by

$$y_{p,m}(n) = \sum_{l=1}^{L} h_{p,m}(l,n) x_p(n+1-l) + v_{p,m}(n),$$
$$n = -N_c+1, \cdots, N; \quad p = 1, 2, \cdots, N_b \quad (1)$$

where $v_{p,m}(n)$ is the additive white Gaussian noise with average power σ^2, L is the length of the frequency-selective fading channel, $h_{p,m}(l,n)$ is the baseband equivalent channel impulse response of the composite fading channel of the m-th branch. The composite channel is the cascade of the transmit pulse shaping filter, air-link fading channel, and the receive matched filter [23].

It is a common practice to choose CP of length N_c such that $N_c \geq L-1$ and

$$x_p(n) = x_p(n+N), \qquad n = -N_c+1, \cdots, -1, 0. \quad (2)$$

After the received signals corresponding to the CP $\{x_p(n)\}_{n=-N_c+1}^{0}$ are removed at the receiver, the received N-point data symbols can be expressed in a matrix form as

$$\mathbf{y}_{p,m} = \mathbf{T}_{p,m}\mathbf{x}_p + \mathbf{v}_{p,m} \quad (3)$$

where

$$\mathbf{y}_{p,m} = \left[\, y_{p,m}(1) \;\; y_{p,m}(2) \;\; \cdots \;\; y_{p,m}(L) \;\; \cdots \;\; y_{p,m}(N) \,\right]^t \quad (4)$$
$$\mathbf{x}_p = \left[\, x_p(1) \;\; x_p(2) \;\; \cdots \;\; x_p(L) \;\; \cdots \;\; x_p(N) \,\right]^t \quad (5)$$
$$\mathbf{v}_{p,m} = \left[\, v_{p,m}(1) \;\; v_{p,m}(2) \;\; \cdots \;\; v_{p,m}(L) \;\; \cdots \;\; v_{p,m}(N) \,\right]^t \quad (6)$$

with $(\cdot)^t$ being the transpose operation, and the time-domain channel matrix is given by (7) at the top of next page.

It is worth noting that, for a general time-varying frequency-selective fading channel, the channel impulse response $h_{p,m}(l,n)$ is varying at each time instant n, and the time-domain channel matrices $\{\mathbf{T}_{p,m}\}_{m=1}^{M}$ is not circulant. In principle, if the receiver has perfect knowledge about the channel response, then the p-th block transmitted data $\mathbf{x}_p$ can be estimated and detected via the minimum mean square error (MMSE) criterion. The standard solution is given by

$$\hat{\mathbf{x}}_p = \left[\sum_{i=1}^{M} \mathbf{T}_{p,m}^h \mathbf{T}_{p,m} + \sigma^2 \mathbf{I}_N\right]^{-1} \left[\sum_{i=1}^{M} \mathbf{T}_{p,m}^h \mathbf{y}_{p,m}\right] \quad (8)$$

where $(\cdot)^h$ is the conjugate transpose operation.

However, this time-domain MMSE equalizer requires the inversion of an $N \times N$ Hermitian matrix that needs $\mathcal{Q}(N^2)$ operations, where N is normally chosen to be large to achieve better data efficiency $\frac{N\cdot(N_b-1)}{(N+N_c)N_b}$. For a large channel length L on the order of several tens, N is usually on the order of hundreds. This can make the time-domain MMSE equalization prohibitively complex.

$$\mathbf{T}_{p,m} = \begin{bmatrix} h_{p,m}(1,1) & 0 & \cdots & 0 & h_{p,m}(L,N{+}1) & \cdots & h_{p,m}(2,N{+}1) \\ h_{p,m}(2,2) & h_{p,m}(1,2) & 0 & \ddots & \ddots & \ddots & \vdots \\ \vdots & \ddots & \ddots & \ddots & \ddots & \ddots & h_{p,m}(L,N{+}L{-}1) \\ h_{p,m}(L,L) & \ddots & \ddots & h_{p,m}(1,L) & 0 & \ddots & 0 \\ 0 & h_{p,m}(L,L{+}1) & \ddots & \ddots & \ddots & \ddots & \vdots \\ \vdots & \ddots & \ddots & \ddots & \ddots & \ddots & 0 \\ 0 & \cdots & 0 & h_{p,m}(L,N) & \cdots & \cdots & h_{p,m}(1,N) \end{bmatrix}. \quad (7)$$

B. Frequency-Domain System Model

Let $\mathbf{F}$ be the normalized FFT matrix of size $N \times N$, whose (k,n)-th element is given by $\frac{1}{\sqrt{N}} \exp\left(\frac{-j2\pi(k-1)(n-1)}{N}\right)$. Taking the FFT of the transmitted and received signals and noticing that $\mathbf{F}^h\mathbf{F} = \mathbf{I}_N$, we can obtain the frequency-domain representation as follows

$$\begin{aligned}\mathbf{Y}_{p,m} \triangleq\ \mathbf{F}\mathbf{y}_{p,m} &= \mathbf{F}\mathbf{T}_{p,m}\mathbf{F}^h\mathbf{F}\mathbf{x}_p + \mathbf{F}\mathbf{v}_{p,m} \\ &= \mathbf{H}_{p,m}\mathbf{X}_p + \mathbf{V}_{p,m} \qquad (9)\end{aligned}$$

where $\mathbf{H}_{p,m} = \mathbf{F}\mathbf{T}_{p,m}\mathbf{F}^h$ is the frequency-domain channel matrix for the p-th block at the m-th branch. The frequency-domain MMSE equalization is given by [18], [19]

$$\hat{\mathbf{X}}_p = \left[\sum_{i=1}^{M} \mathbf{H}_{p,m}^h \mathbf{H}_{p,m} + \sigma^2 \mathbf{I}_N\right]^{-1} \left[\sum_{i=1}^{M} \mathbf{H}_{p,m}^h \mathbf{Y}_{p,m}\right]. \quad (10)$$

For general time-varying and frequency-selective fading channels, the time-domain channel matrix $\mathbf{T}_{pi}$ is not circulant and frequency-domain channel matrix $\mathbf{H}_{p,m}$ is not diagonal. Therefore, the frequency-domain MMSE equalization (10) has no advantage over its time-domain counterpart in terms of computational complexity, because the frequency tones of the received signal $\mathbf{Y}_{p,m}$ are not orthogonal.

However, if the block time duration T_b is much smaller than the channel coherence time, *i.e.*, the fading channel coefficients remains approximately constant for the entire block, then $\mathbf{T}_{p,m}$ is circulant and $\mathbf{H}_{p,m}$ is diagonal. Consequently, the frequency tones $\{Y_{p,m}(k)\}_{k=1}^{N}$ of the received signal are orthogonal and the frequency-domain input-output relationship and equalization are simplified as

$$Y_{p,m}(k) = H_{p,m}(k)X_p(k) + V_{p,m}(k), \quad k = 1, 2, \cdots, N \quad (11)$$

$$\hat{X}_p(k) = \left[\sum_{i=1}^{M} |H_{p,m}(k)|^2 + \sigma^2\right]^{-1} \left[\sum_{i=1}^{M} H_{p,m}^h(k) Y_{p,m}(k)\right], \quad k = 1, 2, \cdots, N \quad (12)$$

where $Y_{p,m}(k)$, $X_p(k)$ and $V_{p,m}(k)$ are the normalized DFT of the corresponding time-domain signals

$$Y_{p,m}(k) = \frac{1}{\sqrt{N}} \sum_{n=1}^{N} y_{p,m}(n) \exp\left(\frac{-j2\pi(n-1)(k-1)}{N}\right) \quad (13)$$

$$X_p(k) = \frac{1}{\sqrt{N}} \sum_{n=1}^{N} x_p(n) \exp\left(\frac{-j2\pi(n-1)(k-1)}{N}\right) \quad (14)$$

$$V_{p,m}(k) = \frac{1}{\sqrt{N}} \sum_{n=1}^{N} v_{p,m}(n) \exp\left(\frac{-j2\pi(n-1)(k-1)}{N}\right) \quad (15)$$

and $H_{p,m}(k)$ is the DFT of the time-domain channel response at the time instant $n = N/2$

$$H_{p,m}(k) = \sum_{l=1}^{L} h_{p,m}(l, \frac{N}{2}) \exp\left(\frac{-j2\pi(l-1)(k-1)}{N}\right). \quad (16)$$

In this case, frequency-domain channel estimation and equalization based on (11) can result in great computational savings over time-domain methods when the channel length L is larger than 10 and the FFT algorithm is employed [7]. In this paper, new algorithms for frequency-domain channel estimation and channel equalization will be developed based on (11). Besides, we will show that our proposed method based on this approximation also works well for time-varying fading channels that have high Doppler frequencies due to high-speed mobile users.

III. Frequency-Domain Channel Estimation

In this section, we employ interpolation method to develop least-squares (LS)-based channel estimation algorithm and MMSE-based channel estimation algorithm in the frequency domain, we show that both algorithms are equivalent. We further present a simplified algorithm for Rayleigh fading channels.

A. LS-Based Frequency-Domain Channel Estimation

For the training block, $p = 1$, both the transmitted training signal $X_1(k)$ and received signal $Y_{1,m}(k)$ are known. The frequency-domain channel transfer function $H_{1,m}(k)$ at the training block can be estimated by LS criterion as follows:

$$\tilde{H}_{1,m}(k) = \frac{Y_{1,m}(k)}{X_1(k)} = H_{1,m}(k) + \frac{V_{1,m}(k)}{X_1(k)}, \quad k = 1, 2, \cdots, N. \quad (17)$$

The estimate $\tilde{H}_{1,m}(k)$ can be improved by a frequency-domain filter to reduce noise. Although various frequency-domain filters can be employed, a common technique is to transform $\tilde{H}_{1,m}(k)$ into the time domain with an IFFT, and use an L-size window mask to remove the noise beyond the channel length, then transform the time-domain channel coefficients back to the frequency domain with an FFT. This procedure was originally proposed in OFDM systems in [21]. The noise-reduced channel estimation of the training block can be represented by

$$\hat{H}_{1,m}(k) = H_{1,m}(k) + \frac{\hat{V}_{1,m}(k)}{X_1(k)}, \quad k = 1, 2, \cdots, N. \tag{18}$$

where $\hat{V}_{1,m}(k)$ is equal to $\frac{1}{\sqrt{N}} \sum_{n=1}^{L} v_{1,m}(n) \exp\left(\frac{-j2\pi(n-1)(k-1)}{N}\right)$.

Provided $v_{1,m}(n)$ is AWGN with average power σ^2, one can easily conclude that $V_{1,m}(k)$ and $\hat{V}_{1,m}(k)$ are zero-mean Gaussian with average power being σ^2 and $\frac{\sigma^2 L}{N}$, respectively, if $X_1(k)$ are constant in the frequency domain. Therefore, the noise average power is reduced by a factor $\frac{N}{L}$ via the FFT-based frequency-domain filter.

Apparently, LS-based channel estimation at the training blocks is straightforward. Although we approximate channel coefficients within a single block as constants, channel coefficients do vary from block to block. Therefore, channel coefficients at the data blocks need to be estimated from the channel transfer functions of the training blocks. We employ interpolation method to develop an algorithm for data block channel estimation that utilizes the estimated channel transfer functions of the current-frame training block and the next-frame training block.

Let $\hat{H}_{N_b+1,m}(k)$ be the noise-reduced channel transfer function estimate of the training block of the next frame, utilizing $X_{N_b+1}(k) = X_1(k)$ for the training signals, then we have

$$\hat{H}_{N_b+1,m}(k) = H_{N_b+1,m}(k) + \frac{\hat{V}_{N_b+1,m}(k)}{X_1(k)} \qquad k = 1, 2, \cdots, N \tag{19}$$

where $\hat{V}_{N_b+1,m}(k)$ is defined similarly to $\hat{V}_{1,m}(k)$.

Define a column vector $\hat{\mathbf{P}}_m(k) = \left[\ \hat{H}_{1,m}(k) \quad \hat{H}_{N_b+1,m}(k)\ \right]^t$. Let $\mathbf{C}_{p,m}(k)$ be the interpolation row vector for the p-th data block in the current frame at the m-th receive branch. Then the proposed method estimates the channel transfer function of the p-th data block in the current frame by

$$\hat{H}_{p,m}(k) = \mathbf{C}_{p,m}(k)\hat{\mathbf{P}}_m(k), \qquad p = 1, 2, \cdots, N_b \tag{20}$$

and the estimation error for the m-th receive branch is given by

$$\begin{aligned} E_{p,m}(k) &= H_{p,m}(k) - \hat{H}_{p,m}(k) \\ &= H_{p,m}(k) - \mathbf{C}_{p,m}(k)\hat{\mathbf{P}}_m(k). \end{aligned} \tag{21}$$

The interpolation vector $\mathbf{C}_{p,m}(k)$ can be designed by minimizing the mean square estimation error $\varepsilon_{p,m}(k) = \mathcal{E}\left\{\left|H_{p,m}(k) - \hat{H}_{p,m}(k)\right|^2\right\}$. The optimal solution for $\mathbf{C}_{p,m}(k)$ can be expressed as (22) on the top of next page.

Substituting (22) and $\hat{\mathbf{P}}_m^h(k)$ into (20), we obtain the LS-based channel estimate $\hat{H}_{p,m}(k)$.

It is noted from (22) that the interpolation vector is determined by the second-order statistics of the channel coefficients rather than the instantaneous channel coefficients.

B. MMSE-Based Frequency-Domain Channel Estimation

In this subsection, we present the minimum mean square error (MMSE)-based channel estimation and prove it is the same as the LS-based channel estimation under certain conditions.

The frequency-domain channel transfer function $H_{1,m}(k)$ at the training block can be estimated by minimum mean square error (MMSE) criterion as follows:

$$\begin{aligned} \check{H}_{1,m}(k) &= \frac{X_1^*(k)Y_{1,m}(k)}{|X_1(k)|^2 + \sigma^2} \\ &= \frac{|X_1(k)|^2}{|X_1(k)|^2 + \sigma^2} H_{1,m}(k) + \frac{X_1^*(k)V_{1,m}(k)}{|X_1(k)|^2 + \sigma^2}. \end{aligned} \tag{23}$$

Similar to the LS-based frequency-domain channel estimation, we can employ the IFFT and FFT to reduce noise beyond the channel length and obtain the noise-reduced channel estimation of the training block given by

$$\begin{aligned} \check{H}_{1,m}(k) &= \frac{X_1^*(k)Y_{1,m}(k)}{|X_1(k)|^2 + \sigma^2} \\ &= \frac{|X_1(k)|^2}{|X_1(k)|^2 + \sigma^2} H_{1,m}(k) + \frac{X_1^*(k)\hat{V}_{1,m}(k)}{|X_1(k)|^2 + \sigma^2}. \end{aligned} \tag{24}$$

Let $\check{\mathbf{P}}_{MMSE}(k) = \left[\ \check{H}_{1,m}(k) \quad \check{H}_{N_b+1,m}(k)\ \right]^t$ be the column vector as the estimated transfer functions at training blocks of the current frame and next frame, and $\mathbf{C}_{MMSE}(p, m, k)$ be the row vector as the corresponding coefficients for the p-th block in the current frame. Then the estimated transfer function of the p-th block of the current frame is given by

$$\check{H}_{p,m}(k) = \mathbf{C}_{MMSE}(p, m, k)\check{\mathbf{P}}_{MMSE}(k) \tag{25}$$

and the estimation error is given by

$$\begin{aligned} \check{E}_{p,m}(k) &= H_{p,m}(k) - \check{H}_{p,m}(k) \\ &= H_{p,m}(k) - \mathbf{C}_{MMSE}(p, m, k)\check{\mathbf{P}}_{MMSE}(k). \end{aligned} \tag{26}$$

The optimal solution for $\mathbf{C}_{MMSE}(p, m, k)$ to minimize the mean square estimation error is given by (27) at next page.

Substituting $\mathbf{C}_{MMSE}(p)$ into eqn. (25), we obtain (28) given next page.

Apparently, one can conclude that the MMSE-based channel estimation $\check{H}_{p,m}(k)$ is exactly the same as the LS-based channel estimation $\hat{H}_{p,m}(k)$ given by eqn. (20) along with (19) and (22).

However, as can be seen from (17) and (23), the LS-based channel estimation is more computationally efficient than the MMSE-based algorithm. Therefore, in the sequel, we will focus on the LS-based channel estimation because of its simplicity. According to (19), a desired property of the training sequence is to have constant $|X_1(k)|^2$ for all m,

$$\mathbf{C}_{p,m}(k)= \mathcal{E}\left\{H_{p,m}(k)\hat{\mathbf{P}}_m^h(k)\right\}\left[\mathcal{E}\left\{\hat{\mathbf{P}}_m(k)\hat{\mathbf{P}}_m^h(k)\right\}\right]^{-1}$$
$$= \left[\mathcal{E}\{H_{p,m}(k)H_{1,m}^*(k)\} \;\; \mathcal{E}\{H_{p,m}(k)H_{N_b+1,m}^*(k)\}\right]\begin{bmatrix}\mathcal{E}\left\{|H_{1,m}(k)|^2\right\}+\frac{\sigma^2 L}{N|X_1(k)|^2} & \mathcal{E}\{H_{1,m}(k)H_{N_b+1,m}^*(k)\}\\ \mathcal{E}\{H_{N_b+1,m}(k)H_{1,m}^*(k)\} & \mathcal{E}\left\{|H_{N_b+1,m}(k)|^2\right\}+\frac{\sigma^2 L}{N|X_1(k)|^2}\end{bmatrix}^{-1}. \quad (22)$$

$$\begin{aligned}\mathbf{C}_{MMSE}(p,m,k) &= \mathcal{E}\left\{H_{p,m}(k)\check{\mathbf{P}}_{MMSE}(k)\right\}\left[\mathcal{E}\left\{\check{\mathbf{P}}_{MMSE}(k)\check{\mathbf{P}}_{MMSE}^h(k)\right\}\right]^{-1}\\ &= \frac{|X_1(k)|^2+\sigma^2}{|X_1(k)|^2}\left[\; \mathcal{E}\left\{H_{p,m}(k)H_{1,m}^*(k)\right\} \quad \mathcal{E}\left\{H_{p,m}(k)H_{N_b+1,m}^*(k)\right\}\;\right]\\ &\quad\times\begin{bmatrix}\mathcal{E}\left\{|H_{1,m}(k)|^2\right\}+\frac{\sigma^2 L}{N|X_1(k)|^2} & \mathcal{E}\left\{H_{1,m}(k)H_{N_b+1,m}^*(k)\right\}\\ \mathcal{E}\left\{H_{N_b+1,m}(k)H_{1,m}^*(k)\right\} & \mathcal{E}\left\{|H_{N_b+1,m}(k)|^2\right\}+\frac{\sigma^2 L}{N|X_1(k)|^2}\end{bmatrix}^{-1}.\end{aligned} \quad (27)$$

$$\begin{aligned}\check{H}_{p,m}(k) &= \left[\; \mathcal{E}\left\{H_{p,m}(k)H_{1,m}^*(k)\right\} \quad \mathcal{E}\left\{H_{p,m}(k)H_{N_b+1,m}^*(k)\right\}\;\right]\\ &\times\begin{bmatrix}\mathcal{E}\left\{|H_{1,m}(k)|^2\right\}+\frac{\sigma^2 L}{N|X_1(k)|^2} & \mathcal{E}\left\{H_{1,m}(k)H_{N_b+1,m}^*(k)\right\}\\ \mathcal{E}\left\{H_{N_b+1,m}(k)H_{1,m}^*(k)\right\} & \mathcal{E}\left\{|H_{N_b+1,m}(k)|^2\right\}+\frac{\sigma^2 L}{N|X_1(k)|^2}\end{bmatrix}^{-1}\begin{bmatrix}H_{1,m}(k)+\frac{\hat{V}_{1,m}(k)}{X_1(k)}\\ H_{N_b+1,m}(k)+\frac{\hat{V}_{N_b+1,m}(k)}{X_1(k)}\end{bmatrix}.\end{aligned} \quad (28)$$

$$\mathbf{C}_p(k) = \begin{bmatrix} J_0\left[2\pi f_d(p-1)T_b\right]\\ J_0\left[2\pi f_d\left(N_b+1-p\right)T_b\right]\end{bmatrix}^t\begin{bmatrix}1+\frac{\sigma^2 L}{N f_h(k)} & J_0\left(2\pi f_d N_b T_b\right)\\ J_0\left(2\pi f_d N_b T_b\right) & 1+\frac{\sigma^2 L}{N f_h(k)}\end{bmatrix}^{-1} \quad (29)$$

$$\varepsilon_p(k) = f_h(k)-f_h(k)\begin{bmatrix} J_0\left[2\pi f_d(p-1)T_b\right]\\ J_0\left[2\pi f_d\left(N_b+1-p\right)T_b\right]\end{bmatrix}^t\begin{bmatrix}1+\frac{\sigma^2 L}{N f_h(k)} & J_0(2\pi f_d N_b T_b)\\ J_0(2\pi f_d N_b T_b) & 1+\frac{\sigma^2 L}{N f_h(k)}\end{bmatrix}^{-1}\begin{bmatrix} J_0\left[2\pi f_d p T_b\right]\\ J_0\left[2\pi f_d\left(N_b-p\right)T_b\right]\end{bmatrix} \quad (30)$$

so that noise amplification on certain frequency tones can be avoided. Although many sequences can achieve this property, a good solution is to adopt Chu sequences [22] as the training sequence, because Chu sequences have constant magnitude in both frequency domain and time domain, which avoids the peak-to-average power ratio problem at the transmitter. In this paper, we choose Chu sequences as the training sequence to ensure $|X_1(k)|^2 = 1$.

C. Simplified LS-Based Channel Estimation for Rayleigh Fading Channels

We are now in a position to present simplified formula for the interpolation vector.

Proposition 1: For frequency-selective Rayleigh fading, the interpolation row vector $\mathbf{C}_{p,m}(k)$ and the minimum mean square error of the LS-based channel estimation are independent from the branch index m, they are given by (29) and (30) at the middle of this page, where $J_0(\cdot)$ is the zero-order Bessel function of the first kind, f_d is the maximum Doppler frequency, and $f_h(k)$ is given by

$$f_h(k) = \sum_{l_1=1}^{L}\sum_{l_2=1}^{L} C_{l_1,l_2}\exp\left(\frac{-j2\pi(l_1-l_2)(k-1)}{N}\right) \quad (31)$$

with C_{l_1,l_2} being the inter-tap correlation of l_1-th tap and l_2-th tap of the fading channel, details are given in [23].

Proof: Details are omitted for brevity.

Remark 1: Interpolation-based channel estimation methods have been previously studied for OFDM systems [25] and for frequency flat fading channels [26], [27], with different channel conditions. In this paper, we consider the discrete-time channel taps have inter-tap correlations, which is the general case [23]. The algorithm presented in this paper is to demonstrate that the interpolation-based channel estimation can deal with much higher Doppler than the existing LMS and RLS algorithms for single-carrier broadband wireless systems.

Remark 2: It is noted that for Rayleigh fading channels, once N_b and T_b are chosen, $\mathbf{C}_p(k)$ is depending on the maximum Doppler frequency f_d and the noise average power σ^2. The estimation of f_d can be done by the algorithm presented in [24] and the estimation of σ^2 can be done by using the time-domain signal components beyond the channel length after performing IFFT when the block length is larger than the channel length.

Remark 3: It is also noted that if the frequency selective fading channel has no inter-tap correlations, *i.e.*, $C_{l_1,l_2} = 0$ for $l_1 \neq l_2$, then $f_h(k) \equiv 1$ for all k. In this case, both $\mathbf{C}_p(k)$ and $\varepsilon_p(k)$ will be independent from the frequency tone k.

Remark 4: Intuitively, the proposed interpolation method computes the channel coefficients of the p-th data block as a weighted sum of the channel coefficients of the two neighboring train blocks. When the block index p is small, its correlation with the training block is stronger than its correlation with $\hat{H}_{N_b+1,m}(k)$. Thus the channel coefficients are mainly determined by $\hat{H}_{1,m}(k)$. When the block index p is large, on the other hand, its channel is highly correlated with the training block of the next frame and is less correlated with the training block of the current frame. Then the channel coefficients of this data block are dominant by the coefficients of the training block of the next frame.

IV. Frequency-Domain Channel Equalization

According to eqn. (11), the p-th block received signals at the M receive branches are given in frequency domain as follows:

$$\begin{bmatrix} Y_{p,1}(k) \\ Y_{p,2}(k) \\ \vdots \\ Y_{p,M}(k) \end{bmatrix} = \begin{bmatrix} H_{p,1}(k) \\ H_{p,2}(k) \\ \vdots \\ H_{p,M}(k) \end{bmatrix} X_p(k) + \begin{bmatrix} V_{p,1}(k) \\ V_{p,2}(k) \\ \vdots \\ V_{p,M}(k) \end{bmatrix}. \quad (32)$$

This equation can be written in a compact form as follows:

$$\mathbf{Y}_p(k) = \mathbf{H}_p(k)X_p(k) + \mathbf{V}_p(k). \quad (33)$$

We are now in a position to state the following result.

Proposition 2: The output of the frequency-domain MMSE equalizer is given by

$$\hat{X}_p(k) = \left[\hat{\mathbf{H}}_p^h(k)\hat{\mathbf{H}}_p(k) + \varepsilon_p(k) + \sigma^2\right]^{-1} \hat{\mathbf{H}}_p^h(k)\mathbf{Y}_p(k), \quad k = 1, 2, \cdots, N \quad (34)$$

where $\hat{\mathbf{H}}_p(k) = \begin{bmatrix} \hat{H}_{p,1}(k) & \hat{H}_{p,2}(k) & \cdots & \hat{H}_{p,n_R}(k) \end{bmatrix}^t$ is the noise-reduced estimated transfer function vector of the p-th block.

Proof: From (21) we have $\mathbf{H}_p(k) = \hat{\mathbf{H}}_p(k) + \mathbf{E}_p(k)$ with $\mathbf{E}_p(k) = \begin{bmatrix} E_{p,1}(k) & E_{p,2}(k) & \cdots & E_{p,n_R}(k) \end{bmatrix}^t$ being the estimation error vector. Replacing $\mathbf{H}_p(k)$ by $\hat{\mathbf{H}}_p(k) + \mathbf{E}_p(k)$, (33) yields

$$\mathbf{Y}_p(k) = \hat{\mathbf{H}}_p(k)X_p(k) + \mathbf{E}_p(k)X_p(k) + \mathbf{V}_p(k). \quad (35)$$

Let $\mathbf{W}_p(k)$ be the frequency-domain equalizer row vector, the output of the equalizer is given by $\hat{X}_p(k) = \mathbf{W}_p(k)\mathbf{Y}_p(k)$. The equalization error vector is given by

$$E_{X_p}(k) = X_p(k) - \hat{X}_p(k) = X_p(k) - \mathbf{W}_p(k)\mathbf{Y}_p(k). \quad (36)$$

Adopting MMSE criterion, we find the equalizer row vector given by

$$\begin{aligned} \mathbf{W}_p(k) &= \mathcal{E}\left\{X_p(k)\mathbf{Y}_p^h(k)\right\}\left[\mathcal{E}\left\{\mathbf{Y}_p(k)\mathbf{Y}_p^h(k)\right\}\right]^{-1} \\ &= \mathcal{E}\{X_p(k)X_p^*(k)\}\hat{\mathbf{H}}^h(k)\Big[\mathcal{E}\{X_p(k)X_p^*(k)\}\hat{\mathbf{H}}(k)\hat{\mathbf{H}}^h(k) \\ &\quad + \mathcal{E}\{X_p(k)X_p^*(k)\}\mathcal{E}\left\{\mathbf{E}_p(k)\mathbf{E}_p^h(k)\right\} + \mathcal{E}\left\{\mathbf{V}_p(k)\mathbf{V}_p^h(k)\right\}\Big]^{-1} \\ &= \hat{\mathbf{H}}^h(k)\left[\hat{\mathbf{H}}(k)\hat{\mathbf{H}}^h(k) + \varepsilon_p(k)\mathbf{I}_{n_R} + \sigma^2\mathbf{I}_{n_R}\right]^{-1} \\ &= \left[\hat{\mathbf{H}}^h(k)\hat{\mathbf{H}}(k) + \varepsilon_p(k) + \sigma^2\right]^{-1}\hat{\mathbf{H}}^h(k) \end{aligned} \quad (37)$$

where the last equality is obtained by using the matrix inversion lemma [28]. This completes the proof.

Finally, applying IFFT on the frequency domain equalized data sequence $\hat{X}_p(k)$, $k = 1, 2, \cdots, N$, we obtain the p-th block estimated data sequence $\hat{x}_p(n)$, $n = 1, 2, \cdots, N$ in the time-domain.

Remark 5: It should be noted that our frequency-domain channel equalizer given by (37) differs from existing ones by taking into consideration of the mean square error $\varepsilon_p(k)$ of the channel interpolation (30). As a matter of fact that most existing techniques are utilizing LMS and/or RLS algorithms to track the channel variations, however, the tracking error statistics are omitted from their equalization algorithms.

Remark 6: In practice, σ^2 is replaced by its estimate $\hat{\sigma}^2$ and $\varepsilon_p(k)$ is calculated by (30) with the estimated Doppler f_d and $\hat{\sigma}^2$.

V. Simulation Results

The performance evaluation of the proposed algorithms has been carried out by extensive computer simulations with various system parameters and fading channels. For comparison purpose, we present numerical examples based on three previously reported wireless systems. The first example is to show that our algorithm provides very good results for fading channels having long delay spread and high Doppler spread. The second and third examples are designed to show that our new algorithm outperforms two recently developed RLS and LMS algorithms which are capable of dealing with moderate time-varying frequency selective fading channels. We employed the improved Clarke's model [29] to carry out all the simulations.

Example 1: we adopt the 60-tap frequency-selective Rayleigh fading channel, where the average power of the first 20 taps ramps up linearly and the last 40 taps ramps down linearly, as described in [5], and the fading channel is normalized to have total average power as one. We choose FFT size $N = 256$, symbol interval $T_s = 0.25\mu s$ and QPSK modulation, which are the same as these of [5]. We further choose frame length $N_f = 10$ to have the same data efficiency as that of [5] for the LMS and RLS adaptations, which employed 10 training blocks at the beginning of every frame and each frame consisted of 100 blocks.

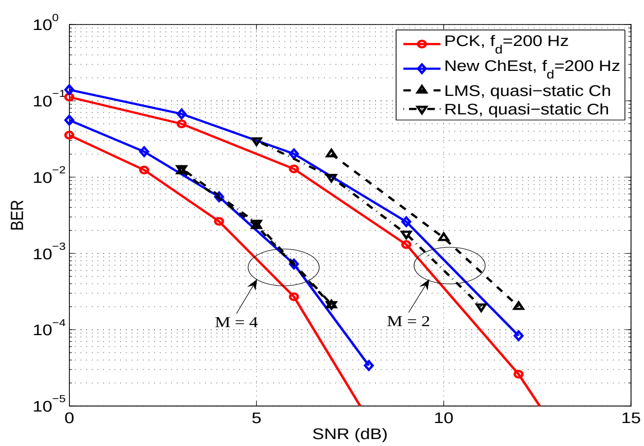

Fig. 3. BER versus SNR of diversity receivers with our proposed algorithms at $f_d = 200$ Hz and those of [5] for quasi-static channel.

Fig. 3 shows the BER performance of a two-antenna receiver and a four-antenna receiver equipped with our proposed

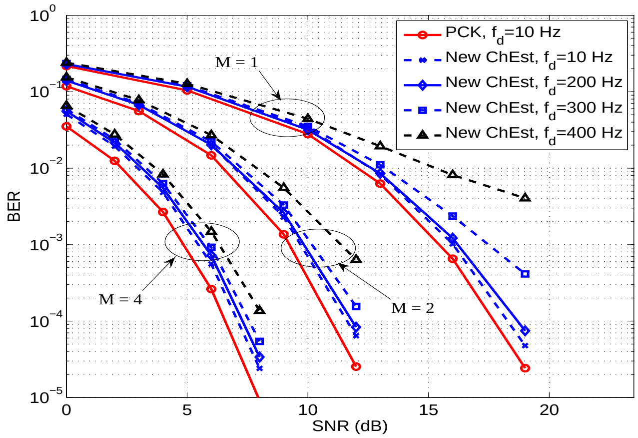

Fig. 4. BER versus SNR of diversity receivers with various Doppler spreads.

algorithms when the Doppler is 200 Hz, which is equivalent to a mobile speed of 114 km/h at carrier frequency of 1.9 GHz. As can be seen, both diversity receivers with our algorithms have only about 1 dB degradation from the ideal receiver with perfect channel fading information. Moreover, for the four-antenna receiver, our algorithm with 200 Hz Doppler has the same performance as the LMS and RLS algorithms of [5] with quasi-static channel, and for the two-antenna receiver, our algorithm with $f_d = 200$ Hz is slightly better than the RLS algorithm but slightly worse than the LMS algorithm of [5] when they are operated with quasi-static channel. The LMS and RLS algorithms will degrade 3-6 dB at BER = 10^{-4} when the Doppler is 200 Hz, as pointed out by the author of [5].

Fig. 4 depicts the BER performance of single-branch receiver, two-branch diversity receiver and four-branch diversity receiver over various Doppler spreads up to 400 Hz. From this figure, it is observed that the BER degradation due to larger Doppler tends to be smaller when the diversity order increases.

Clearly, our proposed algorithms can effectively cope with severe fading channels which has very long impulse response and large Doppler shift.

Example 2: We adopt the same 11-tap frequency-selective Rayleigh fading channel whose l-th tap has average power given by $1.2257\exp(-0.8l)$, as described in [19]. We choose frame length $N_b = 10$, FFT size $N = 128$, CP length $N_c = 10$, symbol interval $T_s = 0.5\mu s$, receive antenna number $M = 1$ and QPSK modulation. Therefore, the data efficiency is $\frac{N}{N+N_c} \times \frac{N_b-1}{N_b} = 83.5\%$, which is slightly higher than the data efficiency of 82.8% in [19].

Figure 5 shows the BER results of the single-branch receiver employing our proposed frequency-domain channel equalization incorporated our proposed noise variance estimation and channel estimation algorithms with various Doppler frequencies $f_d = 20, 50, 100, 200$ and 300 Hz. For comparison purpose, the results of MMSE equalizers based on perfect channel knowledge and RLS adaptive algorithm [19] with normalized Doppler $f_d T_s = 1\times10^{-5}$, *i.e.*, $f_d = 20$ Hz are also included. As can be seen from the BER results, for Doppler frequency up to 50 Hz, our proposed algorithms is less than 1 dB away from the ideal case with perfect channel knowledge at BER of 10^{-5}. For Doppler up to 300 Hz, our algorithms still provide better results than that of the RLS algorithm in [19] with Doppler $f_d = 20$ Hz. This indicates that our algorithm can handle 15 times higher Doppler than the RLS algorithm in [19], and still provides better BER performance and maintains slightly higher data efficiency. The cost we pay for the proposed algorithm is using 128-point FFT and IFFT while the RLS algorithm in [19] employs 64-point FFT and IFFT. However, our channel estimation algorithm has lower computational complexity than the channel tracking algorithm with RLS adaptation.

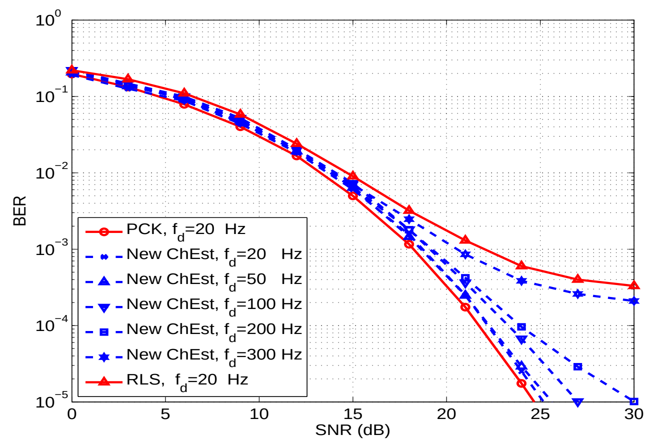

Fig. 5. BER versus SNR of a single-antenna receiver.

Example 3: In [16], several channel estimation methods were proposed. It was shown that when the carrier frequency is 2GHz, mobile speeds are 25, 70 and 140 km/h, symbol interval $T_s = 0.5\mu s$, the LMS structured channel estimation (LMS-SCE) method had the best performance among the methods proposed in [16].

We adopt the same 26-tap frequency-selective Rayleigh fading channel described in [16]. We choose frame length $N_b = 20$, FFT size $N = 128$, CP length $N_c = 25$, symbol interval $T_s = 0.5\mu s$, receive antenna number $M = 1$ and QPSK modulation. Therefore, the data efficiency is $\frac{N}{N+N_c} \times \frac{N_b-1}{N_b} = 79.48\%$, which is the same data efficiency as that of [16].

Figure 6 shows the BER results versus E_b/N_0 of the single-branch receiver employing our proposed frequency-domain channel equalization incorporated our proposed noise variance estimation and channel estimation algorithms with mobile speeds 25, 70 and 140 km/h and carrier frequency 2GHz. For comparison purpose, the results of MMSE equalizers based on perfect channel knowledge and LMS-SCE adaptive algorithm [16] are also included. As can be seen from the BER results, for mobile speed 25 km/h, our new algorithm is slightly better than the LMS-SCE algorithm, for mobile speeds 70 and 140 km/h, our algorithm is 1-5 dB better than the LMS-SCE method.

It should be pointed out that the LMS-SCE method has much higher computational complexity than our method. Because the LMS-SCE method uses $2N$ samples per N data symbols for FFT, channel estimation and channel equalization, while our method uses N points samples, and our interpolation method is more computationally efficient than the LMS-SCE adaptation.

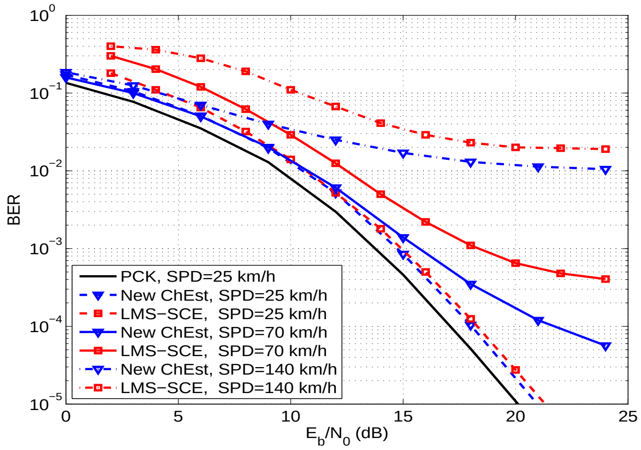

Fig. 6. BER versus E_B/N_0 of a single-antenna receiver.

VI. Conclusion

In this paper, we have presented algorithms for fading channel estimation, noise variance estimation and fading channel equalization in the frequency domain for single carrier broadband wireless communications. It was shown that the LS-based channel estimation and MMSE-based channel estimation with interpolations are equivalent. It has been demonstrated via examples that the proposed algorithms perform very well for broadband wireless communication systems which encounter long impulse response and fast time-varying fading channels. Numerical results have shown that our algorithms has 3-6 dB gain over the LMS and/or RLS algorithms in [5] at 200Hz Doppler, and our algorithm can handle 15 times higher Doppler than the RLS algorithm in [19]. Moreover, our algorithm results in lower bitter error rate and less computational complexity than those of [16].

References

[1] T. Walzman and M. Schwartz, "Automatic equalization using the discrete frequency domain," *IEEE Trans. Info. Theory*, vol.IT-19, pp.57-68, 1973.

[2] H. Sari, G. Karam, and I. Jeanclaude, "Frequency-domain equalization of mobile radio and terrestrial broadcast channels," in *Proc. IEEE Global Telecommun. Conf.*, pp.1-5, Nov. 1994.

[3] G. Kadel, "Diversity and equalization in frequency domain–A robust and flexible receiver technology for broadband mobile communication systems," in *Proc. IEEE Veh. Technol. Conf.*, pp.894-898, May 1997.

[4] A. Czylwik, "Comparison between adaptive OFDM and single carrier modulation with frequency domain equalization," in *Proc. IEEE Veh. Technol. Conf.*, pp.865-869, May 1997.

[5] M. V. Clark, "Adaptive frequency-domain equalization and diversity combining for broadband wireless communications," *IEEE J. Select. Areas Commun.*, vol.16, pp.1385-1395, Oct. 1998.

[6] N. Al-Dhahir, "Single-carrier frequency-domain equalization for space-time block-coded transmissions over frequency-selective fading channels," *IEEE Commun. Lett.*, vol.5, pp.304-306, July 2001.

[7] D. Falconer, S. L. Ariyavisitakul, A. Benyamin-Seeyar, and B. Eidson, "Frequency domain equalization for single-carrier broadband wireless systems," *IEEE Commun. Mag.*, vol.40, no.4, pp.58-66, Apr. 2002.

[8] A. Gusmao and R. Dinis, "On frequency-domain equalization and diversity combining for broadband wireless communications," *IEEE Trans. Commun.*, vol.51, pp.1029-1033, July 2003.

[9] X. Zhu and R. D. Murch, "Layered space-frequency equalization in a single-carrier MIMO system for frequency-selective channels," *IEEE Trans. Wireless Commun.*, vol.3, pp.701-708, May 2004.

[10] K. Takeda, T. Itagaki, and F. Adachi, "Application of space-time transmit diversity to single-carrier transmission with frequency-domain equalisation and receive antenna diversity in a frequency-selective fading channel," *IEE Proc.-Commun.*, vol.151, pp.627-632, Dec. 2004.

[11] Y. Zeng and T. S. Ng, "Pilot cyclic prefixed single carrier communication: channel estimation and equalization," *IEEE Signal Processing Letters*, pp. 56-59, Jan. 2005.

[12] F. Pancaldi and G. M. Vitetta, "Block channel equalization in the frequency domain," *IEEE Trans. Commun.*, vol.53, pp.463-471, March 2005.

[13] Y. Zhu and K. B. Letaief, "Single-carrier frequency-domain equalization with decision-feedback processing for time-reversal space-time block-coded systems," *IEEE Trans. Commun.*, vol.53, pp.1127-1131, Jul. 2005.

[14] K. Takeda and F. Adachi, "SNR estimation for pilot-assisted frequency-domain MMSE channel estimation," *Proc. IEEE VTS APWCS*, Japan, Aug. 2005.

[15] J. Tan and G. L. Stuber, "Frequency-domain equalization for continuous phase modulation," *IEEE Trans. Wireless Commun.*, vol.4, pp.2479-2490, Sept. 2005.

[16] M. Morelli, L. Sanguinetti, and U. Mengali, "Channel estimation for adaptive frequency-domain equalization," *IEEE Trans. Wireless Commun.*, vol.4, pp.2508-2518, Sept. 2005.

[17] N. Benvenuto and S. Tomasin, "Iterative design and detection of a DFE in the frequency domain," *IEEE Trans. Commun.*, vol.53, pp.1867-1875, Nov. 2005.

[18] S. Ahmed, M. Sellathurai, S. Lambotharan, and J. A. Chambers, "Low-complexity iterative method of equalization for single carrier with cyclic prefix in doubly selective channels," *IEEE Sig. Proc. Lett.*, vol.13, pp.5-8, Jan. 2006.

[19] J. Coon, M. Sandell, M. Beach, and J. McGeehan, "Channel and noise variance estimation and traking algorithms for unique-word based single-carrier systems," *IEEE Trans. Wireless Commun.*, vol.5, pp.1488-1496, June 2006.

[20] A. V. Oppenheim, R. W. Schafer, and J. R. Buck, *Discrete-time signal processing*, 2nd Ed., Prentice Hall, 1999.

[21] A. Chini, "Multicarrier modulation in frequency selective fading channels," Ph.D. disserttion, Carleton University, Ottawa, Canada, 1994.

[22] D. C. Chu, "Polyphase codes with good periodic correlation properties," *IEEE Trans. Inform. Theory*, vol.IT-18, pp.531-532, July 1972.

[23] C. Xiao, J. Wu, S.Y. Leong, Y.R. Zheng, and K.B. Letaief, "A discrete-time model for triply selective MIMO Rayleigh fading channels," *IEEE Trans. Wireless Commun.*, vol.3, pp.1678-1688, Sept. 2004.

[24] Y. R. Zheng and C. Xiao, "Mobile speed estimation for broadband wireless communications," in *Proc. IEEE WCNC'07*, Hong Kong, China, 11-15 March 2007.

[25] Y. Li, L.J. Cimini, and N.R. Sollenberger, "Robust channel estimation for OFDM systems with rapid dispersive fading channels," *IEEE Trans. Commun.*, vol.46, pp.902-915, July 1998.

[26] J.K. Cavers, "An analysis of pilot symbol assisted modulation for Rayleigh fading channels," *IEEE Trans. Veh. Technol.*, vol.40, pp.686-693, Nov. 1991.

[27] C. Xiao and J.C. Olivier, "Nonselective fading channel esimation with non-uniformly spaced pilot symbols," *Int. J. Wireless Inform. Netowrks*, vol.7, pp.177-185, July 2000.

[28] R. A. Horn and C. R. Johnson, *Matrix Analysis*, Cambridge University Press, 1985.

[29] C. Xiao, Y.R. Zheng, and N.C. Beaulieu, "Novel sum-of-sinusoids simulation models for Rayleigh and Rician fading channels," *IEEE Trans. Wireless Commun.*, vol.5, pp.3667-3679, Dec. 2006.

PLACE PHOTO HERE

Yahong Rosa Zheng (S'99-M'03-SM'07) received the B.S. degree from the University of Electronic Science and Technology of China, Chengdu, China, in 1987, the M.S. degree from Tsinghua University, Beijing, China, in 1989, both in electrical engineering. She received the Ph.D. degree from the Department of Systems and Computer Engineering, Carleton University, Ottawa, ON, Canada, in 2002.

From 1989 to 1997, she held Engineer positions in several companies. From 2003 to 2005, she was a Natural Science and Engineering Research Council of Canada (NSERC) Postdoctoral Fellow at the University of Missouri, Columbia, MO. Currently, she is an Assistant Professor with the Department of Electrical and Computer Engineering at Missouri University of Science and Technology, Rolla, MO. Her research interests include array signal processing, wireless communications, and wireless sensor networks.

Dr. Zheng is an Editor for the IEEE TRANSACTIONS ON WIRELESS COMMUNICATIONS. She has served as a Technical Program Committee member for a number of IEEE international conferences including SensorsCon, ICC, Globecom and WCNC in the last several years.